

GPipe: Efficient Training of Giant Neural Networks using Pipeline Parallelism

Yanping Huang
Google Brain
huangyp@google.com

Youlong Cheng
Google Brain
ylc@google.com

Dehao Chen
Google
dehao@google.com

HyoukJoong Lee
Google
hyouklee@google.com

Jiquan Ngiam
Google Brain
jngiam@google.com

Quoc V. Le
Google Brain
qvl@google.com

Zhifeng Chen
Google Brain
zhifengc@google.com

Abstract

GPipe is a scalable pipeline parallelism library that enables learning of giant deep neural networks. It partitions network layers across accelerators and pipelines execution to achieve high hardware utilization. It leverages recomputation to minimize activation memory usage. For example, using partitions over 8 accelerators, it is able to train networks that are $25\times$ larger, demonstrating its scalability. It also guarantees that the computed gradients remain consistent regardless of the number of partitions. It achieves an almost linear speed up without any changes in the model parameters: when using $4\times$ more accelerators, training the same model is up to $3.5\times$ faster. We train a 557 million parameters AmoebaNet model and achieve a new state-of-the-art 84.3% top-1 / 97.0% top-5 accuracy on ImageNet. Finally, we use this learned model as a initialization for training 7 different popular image classification datasets and obtain results that exceed the best published ones on 5 of them, including pushing the CIFAR-10 accuracy to 99% and CIFAR-100 accuracy to 91.3%.

1. Introduction

Deep neural networks have advanced many machine learning tasks, including speech recognition [11], visual recognition [56, 44], and language processing [17]. Their success has been largely due to the model’s capacity to learn complex features from vast amounts of data. Increasing the size of models has been shown to dramatically improve task performance. One of the most challenging and popular machine learning tasks is to solve the ImageNet visual recognition challenge [16], where researchers compete

to create the most accurate model that classifies given images in the dataset. The winner of 2014 ImageNet challenge was GoogleNet [48], which achieved 74.8% top-1 accuracy with 4 million parameters. The winner of 2017 ImageNet challenge went to Squeeze-and-Excitation Networks [24], which achieved 82.7% top-1 accuracy with 145.8 million parameters. This corresponds to more than a $36\times$ increase in the number of parameters in the best visual recognition models, as shown in Figure 1. However, memory available on accelerators such as GPUs have only increased from 12 GB in 2014 (Nvidia K40) to 32 GB in 2018 (Nvidia V100). Hence, training even bigger neural networks can be challenging when faced with the accelerator memory limits.

There are increasing needs for scaling up deep neural networks. Modern machine learning datasets are growing faster than ever in terms of dataset size and quality. Image classification datasets such as OpenImages, JFT [46], and hashtagged Instagram [36] contain hundreds of millions of high definition images. Higher image resolutions provides greater details of the object but consumes more memory. This leads to a contention between memory allocated to model parameters and network activations for each example - reinforcing a need for breaking the accelerator memory limit. The larger volume of training data helps reduce overfitting and facilitates deep neural networks to grow bigger. Meanwhile, the emergence of deep learning super computers such as Nvidia DGX and Google TPU enables efficient parallelism by providing fast interconnections between accelerators. We have reached the limits of training a big image model on a single accelerator. The memory restriction has limited the scales of deep neural networks and confined researchers to smaller scale problems with fewer parameters. For example, while the average ImageNet resolution

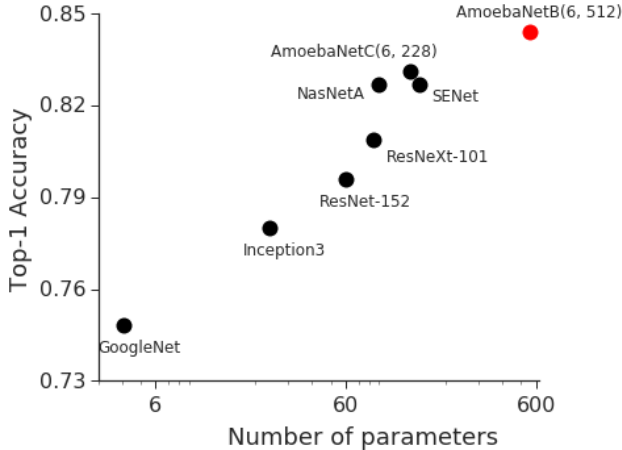


Figure 1: Strong correlation between top-1 accuracy on ImageNet ILSVRC 2012 validation dataset and model size for representative state-of-the-art image classification models in history [48, 49, 23, 52, 24, 56, 44]. Red dot shows 84.3% top-1 accuracy for a giant AmoebaNet model trained by GPipe.

is 469×387 , it has been shown that increasing input image size can lead to higher accuracy [23]. However, most current models are engineered to only use input image size 299×299 or 331×331 to fit within accelerator memory limits. Our work focuses on removing this limiting factor of scaling up deep neural networks.

To overcome the memory limitation, we propose to use pipeline parallelism to scale up deep neural network training. We design and implement GPipe, a distributed machine learning library that uses synchronous mini-batch gradient descent for training. GPipe partitions a model across different accelerators and automatically splits a *mini-batch* of training examples into smaller *micro-batches*. By pipelining the execution across micro-batches, accelerators can operate in parallel. In addition, GPipe automatically recomputes the forward activations during the backpropagation to further reduce the memory consumption. Gradients are consistently accumulated across micro-batches, so that the number of partitions does not affect the model quality. Therefore, GPipe allows researchers to easily deploy more accelerators to train larger models, and also to scale the performance without tuning hyperparameters.

GPipe maximizes memory allocation for model parameters. In experiments, we show that GPipe can support models up to 25 times larger using 8 accelerators without reducing the batch size. The implementation of GPipe is very efficient: with $4\times$ more accelerators we can achieve a $3.5\times$ speedup for training giant neural networks. GPipe can be combined with data parallelism [50] to scale training in a complementary way.

Finally, we demonstrate the empirical power of giant neural networks on image classification tasks. We increased the number of parameters for a AmoebaNet model by 4 times to 557 millions and trained it with input image size of 480×480 on ImageNet ILSVRC 2012 dataset. Our scaled-up AmoebaNet model attained 84.3% top-1 / 97.0% top-5 validation accuracy. To the best of our knowledge, it outperforms all other models trained from scratch on ImageNet dataset. Furthermore, we used this learned giant model as an initialization for training a wide range of seven datasets that span from general recognition to fine-grained classification. We find that the giant models performs well on the those datasets, obtaining results that are exceeding or compare-able to state-of-the-art models. For example, we pushed the CIFAR-10 accuracy to 99% and CIFAR-100 accuracy to 91.3%.

In summary, this paper introduces GPipe, a scalable model parallelism library for training giant deep learning models with the following key contributions:

- It supports models up to $25\times$ using 8 accelerators thanks to recomputation and model parallelism.
- It achieves up to $3.5\times$ speedup with four times more accelerators using pipelining in our experiments.
- It guarantees consistent training regardless of the number of partitions due to synchronous gradient descent.
- It advances the performance of visual recognition tasks on multiple datasets, including pushing ImageNet top-5 accuracy to 97.0%, CIFAR-10 accuracy to 99.0%, and CIFAR-100 accuracy to 91.3%.

2. Related Work

Deep neural networks typically consist of a sequence of layers. During training, a neural network first uses the current model parameters to compute predictions from input mini-batches in the forward pass. Then, the gradients are computed by backpropagating prediction errors (Figure 2a). Computing gradients in each intermediate layer requires both gradients from upper layers and the cached output activations from the forward pass. Thus, activation memory requirements typically grows in proportion to the number of layers, leaving less space for storing model parameters.

Various efforts have been studied to allow accelerators to train bigger models. They come with different trade-offs between memory, performance, and model quality. One common method is to recompute the forward pass activations during backpropagation [21, 8], which significantly reduces memory required to cache activations. However, this method is still limited by the size of a single accelerator memory. Another approach is to swap memory between accelerators and the host [15]. However, this approach often slows down training because of the communication bottleneck.

Standard parallelism techniques including data parallelism and model parallelism provide orthogonal ways to use more accelerators for training. Data parallelism [50] effectively scales up the global mini-batch size. It lets each machine compute the gradient on a mini-batch of training examples. Each machine either synchronously or asynchronously updates the model parameters at the end of each training step [4, 35]. Data parallelism is widely used due to its simplicity and effectiveness. Because the batch size is proportional to the number of machines and different batch sizes often require different hyperparameters, scale-out deep net training purely by data parallelism has become more challenging.

Model parallelism is a complementary technique to data parallelism. A naive strategy is to divide the computation into partitions and assign different partitions to different accelerators [31, 34]. This approach is straightforward when there are parallel branches in the network. However, many deep learning models stack layers sequentially, which presents a challenge to parallelize computation efficiently. A naive partition strategy may result in only one accelerator active during computation, significantly underutilizing accelerator compute capacity (Figure 2b).

Pipelining is a common parallel algorithm [33] that integrates model and data parallelism. Petrowski *et al.* explored accelerating training neural networks via pipelining on early parallel machines [42]. Chen *et al.* used pipeline computation to approximate expensive backpropagation [9]. Wu *et al.* [51] parallelized computation of stacked recurrent neural networks on GPUs in the pipelining way. Recently, PipeDream [22] introduced a pipelining approach to reduce communication overhead for synchronized training using parameter servers [35]. However, it suffers from inconsistency and staleness issues in the backward pass, which could lead to unstable and poor model quality. PipeDream maintains multiple versions of model parameters on the accelerator to address the consistency issue. These constraints can prevent PipeDream from scaling up to bigger models. Similarly, DualPipe [6] optimizes pipeline performance by assuming that there exists a robust way to predict future model parameters for back-propagation. Unlike these approaches, GPipe does not have any inconsistency or staleness issue. It integrates recomputation with pipeline parallelism to maximize memory and compute utilization. It offers effective and efficient synchronous training of large scale deep neural networks.

3. Methods

This section describes main design features of GPipe. This library is implemented using the TensorFlow [1] framework. The core algorithm can be implemented using other frameworks [27, 7, 40] as well. We will be open sourced in the near future.

3.1. Interface

The caller of the GPipe interface specifies a sequential list of L layers. Each layer specifies its model parameters w_i , its stateless forward computation function f_i , and an optional cost estimation function c_i that estimates the static computation cost of i -th layer given shapes of all inputs to the layer. Neighboring layers can be combined into a composite layer. For example, the composite layer p_k may be composed of consecutive layers from the i -th layer to the j -th layer. In this case, p_k 's model parameters would be the union of w_i, w_{i+1}, \dots, w_j and its forward function would be $F_k = f_j \circ \dots \circ f_{i+1} \circ f_i$. The corresponding back-propagation function B_k is derived from F_k using TensorFlow's automatic symbolic differentiation mechanism. Its cost estimator is constructed based on c_i, c_{i+1}, \dots, c_j .

3.2. Algorithm

After users defined their network layers in terms of model parameter w_i , cost estimation function c_i and forward computation function f_i , GPipe partitions the layers into K composite layers and places k -th composite layer onto k -th accelerator, where K is the number of partitions users specified. Communication primitives are automatically inserted by GPipe at the partition boundaries to allow communication between neighboring partitions. The partitioning algorithm is heuristic-based. It simply minimizes the variance of each composite layer's estimated cost. We expect that better partitioning algorithms can potentially improve the performance of GPipe.

During training, GPipe first divides a mini-batch of size N into T micro-batches at the first layer. Each micro-batch contains $\frac{N}{T}$ examples. For instance, an image input tensor with shape $[N, H, W, C]$ is reshaped into $[T, \frac{N}{T}, H, W, C]$. During the forward pass (Figure 2c), the $(k+1)$ -th accelerator starts to compute $F_{k+1,t}$ as soon as it finishes the $(t-1)$ -th micro-batch and receives inputs from $F_{k,t}$. At the same time, the k -th accelerator can start to compute $F_{k,t+1}$. Each accelerator repeats this process T times to finish the forward pass of the whole mini-batch. There are still up to $O(K)$ idle time per accelerator, which refers to *bubble* overhead as depicted in Figure 2c. This bubble time is amortized by the number of micro-batches T . The last accelerator is also responsible for concatenating the outputs across micro-steps and computing the final loss.

During the backward pass, gradients for each micro-batch are computed based on the same model parameters as the forward pass. Gradients are applied to update model parameters across accelerators only at the end of each mini-batch. Therefore, GPipe maintains the same synchronous nature of gradient descent, independent of the number of partitions. This is important because deep learning training is sensitive to hyperparameters such as learning rate schedules and dropout probabilities. Our guarantees frees

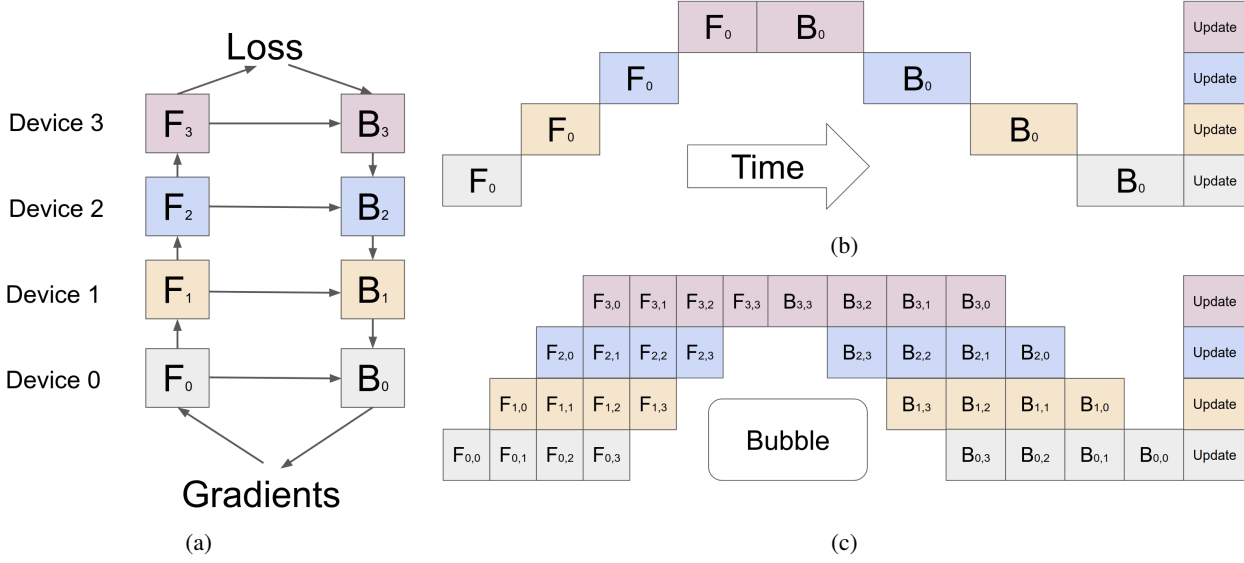


Figure 2: (a) An example neural network with sequential layers is partitioned across four accelerators. F_k is the composite forward computation function of k -th partition. B_k is the corresponding backpropagation function. B_k depends on both B_{k+1} from upper layer and the cached output of F_k . (b) The naive model parallelism strategy leads to severe under-utilization due to the sequential nature of the network. Only one compute accelerator is active at a time. (c) Pipeline parallelism divides the input mini-batch into smaller micro-batches. It enables different accelerators to work on different micro-batches at the same time. $F_{k,t}$ and $B_{k,t}$ refer to forward and backward computation of the t -th micro-batch on k -th partition. Gradients are applied synchronously at the end of each mini-batch.

researchers from the time consuming process of re-tuning hyperparameters.

If batch normalization [25] is used in the network, the sufficient statistics of inputs during training are computed over each *micro-batch*, and over replicas if necessary [41]. We also track the moving average of the sufficient statistics using the entire *mini-batch* for use during evaluation.

3.3. Optimization

The computation of the backward pass $b_i(x)$ at layer i requires both the upper layer gradients $b_{i+1}(x)$ and cached activations $f_i(x)$. Therefore, the total cached activations need $O(N \times L)$ space without optimization. In order to reduce activation memory requirements, GPipe carefully recomputes the forward passes. Each accelerator only stores output activations at the partition boundaries, rather than activations of all intermediate layers within the partition. During the backward pass, the k -th accelerator recomputes the composite forward function F_k and requires only the cache activations at the partition boundaries. As a result, the size of activation memory reduces to $O(N)$, independent of the number of layers L . This reduction becomes significant when training deep networks that have hundreds of layers, which are common in image classification layers.

As depicted in Figure 2c, the aggregation of the loss during the forward pass introduced a bubble of idleness be-

tween the forward and backward passes. The bubble is amortized over the number of micro-steps T . In our experiments, we found that the bubble overhead was quite small. This is because the recomputation during the backward pass can be scheduled earlier without waiting for gradients from earlier layers. Figure 2c assumes partitions are evenly balanced. However, memory requirements and computation flops at different layers are often quite imbalanced. For example, the number of convolution filters doubled every time there is a reduction in spatial dimensions of the activation tensors for many modern image models, such as ResNet, Inception, NasNets, and AmoebaNets. The activation memory footprint per layer decreases linearly at later layers while the number model parameter per layer increases quadratically. Therefore, imperfect partitioning algorithms will lead to load imbalance when partitioning those layers. Better partitioning algorithms can potentially improve the performance over our heuristic approach.

4. Results

This section provides detailed analysis of scalability and performance of GPipe. We evaluated ResNet and AmoebaNet in the experiments. ResNet is a representative neural network for image classification. AmoebaNet was the previous state-of-the-art image model on ImageNet. Both

networks allow us to increase the model size by changing the number of layers or the number of filters. We ran the experiments on TPU-v2s, each of which has 8 accelerator cores and 64 GB memory (8 GB per accelerator).

4.1. Memory

GPipe uses recomputation and pipeline parallelism for better memory utilization. We expect that both methods can enable bigger model, which we verified experimentally in this section. To do this, we fix the input image size at 224×224 and the mini-batch size at 128. We studied the effect of each method on the maximum AmoebaNet model size that would fit with k accelerators, $k \in \{1, 2, 4, 8\}$. An AmoebaNet model consists of a sequence of two repeated layer modules called *normal cell* and *reduction cell*. Normal cell reserves input activation size. Reduction cell reduces the spatial dimension of input but increases the filter size. The size of an AmoebaNet is configured by two hyperparameters, L and F . L defines the number of normal cells stacked between reduction cells and F specifies the number of filters in the first normal cell. We increased L and F until we reached the limits of accelerator memory. We then compared training a model with and without recomputation on a single accelerator to understand the benefits that GPipe introduces. We also partitioned AmoebaNet across different number of accelerators to study the payoff of pipeline parallelism. We reported the maximum model size, the peak activation memory, and peak model parameters memory across accelerators under different scenarios Table 1.

First, we found that recomputation enables $3.8\times$ bigger models. Without recomputation, a single accelerator can train up to 82 million model parameters due to memory limits. Recomputation reduces activation memory from 6.26GB to 3.46GB, enabling 318 million parameters on a single accelerator. For each model parameter, GPipe consumes 12 bytes, i.e., one single precision float for each of the parameter itself, its moving average and momentum.

Second, we saw that with pipeline parallelism the maximum model size is proportional to the number of partitions, as expected. GPipe was capable of enabling AmoebaNet with 1.8 billion parameters across 8 accelerators, a $5.6\times$ increase compared to that on a single accelerator. Combined with recomputation, GPipe supports models that are $25\times$ bigger using 8 accelerators in this experiment. The maximum model size is not a perfect linear function of the number of partitions because of the non-uniform distribution of model parameters over layers in AmoebaNet. This makes it challenging to distribute model parameters evenly across multiple accelerators. With improvements from the partitioning algorithms, GPipe would be capable of allocating even larger models.

4.2. Performance

In this section, we evaluate various factors that trade-off GPipe performance for better memory utilization. For example, recomputation of forward passes reduces activation memory but inevitably introduces computation overhead. Pipeline parallelism partitions networks across accelerators, but it can have overheads such as imbalanced workload and bubbles of idleness. It also requires setup time to divide and reshape the inputs. In our experiments, we measured the effects of pipeline parallelism and recomputation on the model throughput of ResNet-101 and AmoebaNet-D (4, 512). We fixed the image size at 224×224 . We adjusted the mini-batch size to maximize the throughput. To isolate the effects of pipeline parallelism, we used k accelerators to train a model with k partitions. Since training AmoebaNet-D (4, 512) requires at least two accelerators, we report the throughput with respect to no pipelining case with two partitions in Figure 3a. We report throughput of ResNet-101 with respect to the sequential case without recomputation in Figure 3b. To assess the overhead cost, we carefully studied the trace files from ResNet-101 runs to identify key factors that affects performance. We also examined how the effects of these factors change with the number of partitions in Figure 4a and 4b.

We observe that the benefit of pipeline parallelism outweighs the performance overhead introduced. We saw an almost linear speed up in training AmoebaNet-D (4, 512). Compared to the naive approach with two partitions, distributing AmoebaNet-D (4, 512) across four times more accelerators achieved $3.5\times$ speedup. The relative throughput of ResNet-101 using GPipe with one partition is 0.8. Recomputation thus introduced about 25% overhead. As ResNet-101 was distributed across more accelerators, performance increased. It achieved about 3 times speedup with 8 accelerators. In both examples, GPipe provides a way to increase throughput using more accelerators, complementary to the traditional data parallelism approach.

To study opportunities for future performance improvements, we identified key factors that would affect GPipe performance. We measured the times spent on different activities listed in Figure 4a. We showed the distributions of these times for ResNet-101 with 2 and 4 partitions in Figure 4a and 4b, respectively. We find that recomputation time is the main contributor to GPipe overhead, taking up to 23% of the total step time. Another source of overhead was load imbalance. With two partitions, it was only 3.2%, but with four partitions, it rose up to 10.9% overhead. Its increasingly difficult for load balancing with more partitions in the network. Thus finding a good partitioning algorithm can help reduce this overhead in general. The theoretical bubble overhead is $O(\frac{K-1}{T+K-1})$ where K is the number of partitions and T is the number of micro-batches in each mini-batch. The bubble overhead observed bubble overhead is

	Naive-1	Pipeline-1	Pipeline-2	Pipeline-4	Pipeline-8
AmoebaNet-D (L, F)	(6, 208)	(6, 416)	(6, 544)	(12, 544)	(24, 512)
# of Model Parameters	82M	318M	542M	1.05B	1.8B
Total Peak Model Parameter Memory	1.05GB	3.8GB	6.45GB	12.53GB	24.62GB
Total Peak Activation Memory	6.26GB	3.46GB	8.11GB	15.21GB	26.24GB

Table 1: Maximum model size of AmoebaNet supported by GPipe under different scenarios. Naive-1 refers to the sequential version without GPipe. Pipeline- k means k partitions with GPipe using k accelerators. L and F control the number of layers and the number of filters of AmoebaNet. We recorded maximum model size by increasing L and F until we reached the limits of accelerator memory in each scenario. Input image size is 224×224 and the batch size is 128. GPipe divides the mini-batch into 16 micro-batches. It supports up to 1.8 billion parameters with 8 accelerators. Total peak model parameter memory and maximal activation memory across all accelerators are also shown.

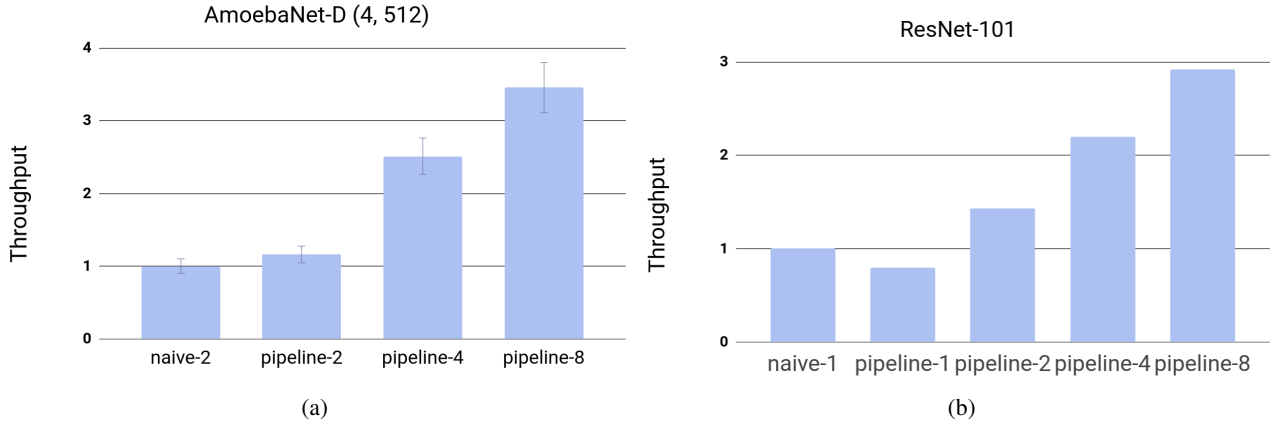


Figure 3: (a): Performance of AmoebaNet-D (4, 512) under different scenarios. This model cannot fit into one accelerator. It achieved 3.5 times speedup comparing to the baseline case naive-2: naive model parallelism with 2 partitions. (b): Performance of ResNet-101 under different scenarios. Pipeline- k means k partitions with GPipe using k accelerators. The baseline naive-1 refers to the sequential version without GPipe. The image size for both models is fixed at 224×224 .

slightly lower than the theoretical value because recomputation is scheduled early to overlap with the bubble. Communication overhead for gradients aggregation at the end of pipeline is negligible thanks to high-speed interconnections between the accelerators.

4.3. Model quality

4.3.1 Consistent Training

GPipe performs synchronous training over the micro-batches. In this section, we verified the hypothesis that the end-to-end convergence accuracy using GPipe is the same within statistical errors, regardless of the number of partitions. We trained AmoebaNet-D (2, 128) several times for 35 epochs and measured the final validation accuracy on ImageNet. We chose AmoebaNet-D (2, 128) since it is the winning image model by training cost in the DAWNBench competition [12]. We adopted the same hyperparameters

and training procedure reported in DAWNBench.¹ As a baseline, we trained AmoebaNet-D (2, 128) 5 times using the official open source implementation and computed the mean and standard deviation of the final accuracy. Using the same hyperparameters and training procedures, we trained the same network using GPipe with 1, 2, 4 and 8 partitions. We found that the resulting accuracy fall within two standard deviations from the mean, as expected.

4.3.2 Scaling up Giant Models

We verified the hypothesis that scaling up existing neural networks can achieve even better model quality. As a proof of concept, we train an AmoebaNet-B (6, 512) with 557 million model parameters and input image size of 480×480

¹https://github.com/stanford-futuredata/dawn-bench-entries/blob/master/ImageNet/train/google_amoeba_net_d_tpu_tensorflow18.json

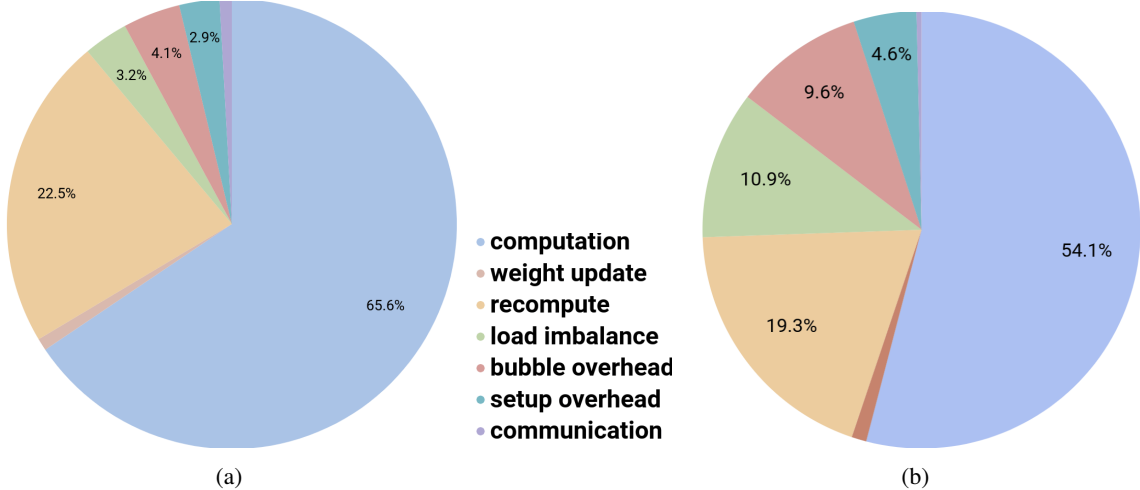


Figure 4: Time step breakdowns from ResNet-101 runs with 2 and 4 partitions, respectively. We analyzed the trace file and measured the times spent on different categories such as pipeline setup, pipeline bubble overhead, load imbalance idle-ness, recomputation, weight update, communication time for gradients aggregation, and the actual computation time for the forward and backward passes.

Model	Image Size	Numbeer of Parameters	Top-1/ top-5 Accuracy (%)
Incep-ResNet V2	299 × 299	55.8M	80.4 / 95.3 [47]
ResNeXt-101	299 × 299	83.6M	80.9 / 95.6 [52]
PolyNet	331 × 331	92.0M	81.3 / 95.8 [54]
Dual-Path-Net-131	320 × 320	79.5M	81.5 / 95.8 [10]
SENet	320 × 320	146M	82.7 / 96.2 [24]
AmoebaNet-C (6, 228)	331 × 331	155.3M	83.5 / 96.5 [13]
AmoebaNet-B (6, 512)	480 × 480	557M	84.3/97.0

Table 2: Top-1 / top-5 classification accuracy for AmoebaNet-B (6, 512) compared to other published state-of-the-art models on ImageNet ILSVRC 2012 validation dataset. Data in the this table suggests that better model quality may be obtained by higher model capacity (# of parameters) and more computation (larger input image size).

on the ImageNet ILSVRC-2012 dataset. We followed the same hyperparameters and input pre-processings as ImageNet models described in [44] to train AmoebaNet-B (6, 512). We employed the RMSProp optimizer with a decay of 0.9 and $\epsilon = 0.1$, L^2 regularization $\lambda = 4 \times 10^{-5}$, label smoothing coefficient 0.1 and an auxiliary head with weight 0.4. We applied the same drop-path schedule to intermediate layers as in NasNet [56], and dropout to the final layer with probability 0.5. We used a learning rate schedule that starts at $0.00125 \times$ batch size and decays every 3 epochs at a rate of 0.97. The network was divided into 4 partitions, and we performed training using both model and data parallelism. We adopted mixed precision training [38] where activations are represented in half precision. Unlike other mixed precision training strategies, we didn't scale the loss values thanks to the wide dynamic range of bfloat16 on

TPUs. We used ImageNet ILSVRC-2012 dataset for training and reported the validation accuracy in table 2. This giant model reached 84.3% top-1 / 97.0% top-5 validation accuracy with single-crop.

4.3.3 Transfer Learning

Large neural networks are applicable to not only datasets like ImageNet, but are also relevant for other datasets through transfer learning [43, 19, 45]. One successful approach to transfer learning is to use ImageNet pre-trained models as an initialization for training on a target dataset. In this section, we evaluate the transfer learning performance for the best giant model found in Section 4.3.2 that achieved 84.3% top-1 accuracy on ImageNet.

We evaluated transfer learning performance on the following datasets: CIFAR-10, CIFAR-100 [32], Birdsnap [2],

Dataset	Our Model (%)	Best Published Result (%)
CIFAR-10	99.0	98.5 [13]
CIFAR-100	91.3	89.3 [13]
Oxford-IIIT Pets	95.9	94.3* [28]
Stanford Cars	94.6	94.1* [53]
Food-101	93.0	90.4* [14]
FGVC Aircraft	92.7	94.5** [30]
Birdsnap	83.6	83.9** [30]

Table 3: Transfer learning results using AmoebaNet-B (6, 512) initialized with the best ImageNet model, using an input image size of 480×480 and single crop at test time. Our results are averaged across 5 fine-tuning runs. (*) We note that Kornblith *et al.* [28], Yu *et al.* [53], and Cui *et al.* [14] also fine-tuned pre-trained weights on ImageNet. (**) Krause *et al.* [30] leverage 9.8 millions additional pre-training images collected using Google image search.

Stanford Cars [29], FGVC Aircraft [37], Oxford-IIIT Pets [39], and Food-101 [3]. This spans a range of tasks from general object recognition to fine-grained classification.

We trained a AmoebaNet-B (6, 512) model for each of these datasets. The classification layer was initialized randomly, while all other layers were initialized with the best parameters on trained on ImageNet. We selected the learning rate and L^2 weight regularization parameters for each dataset using on a hold out validation set. We reused other hyperparameters used in ImageNet training. We adopted image pre-processing procedure that is widely used for training CIFAR datasets. In all our transfer learning experiments, input images to the network during training were resized to 480×480 , horizontally flipped randomly and augmented using cutout [18] for all datasets. We trained the models for 20,000 steps using stochastic gradient descent with Nesterov momentum. Each mini-batch contained 256 examples. We report the averaged single-crop accuracy on test sets across 5 fine-tuning runs for each dataset.

We found that the giant models performs well on the target datasets, obtaining results that are exceeding or comparable to state-of-the-art models in Table 3. For example, our finetuned models reduced CIFAR-10 error rate to 1% and CIFAR-100 error rate to 8.7%. These results corroborated Kornblith *et al.* [28] findings that ImageNet performance correlates well with transfer learning performance.

5. Discussion

Our work reinforced the hypothesis that bigger models and more computation would lead to higher model quality. This hypothesis is also supported by past advances in visual recognition tasks shown in Figure 1 and the recent progresses in other fields such as BigGAN [5] and BERT[17].

Those results suggest that accuracy improvements of machine learning tasks may be obtained by further increases in the scale of neural networks beyond the limits of accelerator memory. Moreover, the availability of bigger datasets such as JFT-300M [46] and hashtagged Instagram [36] also reduced risks of over-fitting and encouraged giant networks with higher capacity.

We scaled up the capacity of AmoebaNet to 557-million parameters by doubling the number of filters. It doesn't mean that it's the most effective way to grow the model size. There might exist better ways for model augmentation like increasing the number of layers or employing more branches of transformations. Actually GPipe supports models up to 2-billion parameters with 8 accelerators in our experiments, inviting future research on searching efficient network architectures with billions of parameters.

Some design choices in the existing neural network architectures might be made by tradeoffs for limited accelerator memory, and need to be revisited when the memory bottleneck is removed. Most existing network architectures aggressively reduce the spatial dimensions of inputs at the beginning in order to decrease activation memory. For example, they employ convolution or pooling with non-unity stride values at the first few layers. Some lower level input features might be omitted because of the aggressive early reductions. Our preliminary results found that delaying reduction significantly improved classification accuracy without increasing the model capacity. In our experiments, we reduced the stride value of the first convolution layer and increased the stride value at the last layer on AmoebaNet-D (2, 256). As a result, the activation memory footprint increased four times but the model size stays the same. The more processing of lower level features allowed the network to increase the ImageNet top-1 accuracy from 78.1% to 82.7%.

GPipe could scale training by employing even more accelerators without changes in the hyperparameters. Therefore, it can be combined with data parallelism to scale neural network training using even more accelerators in a complementary way. Pure data parallelism with stochastic gradient descent runs into inferior model generalization issues when the size of the global mini-batch is extremely large [20, 26]. Significant re-tuning and optimization is required to train on ImageNet without loss of accuracy when the global mini-batch size is greater than $8k$.

GPipe enables pipeline parallelism for any neural networks that consists of sequence of layers. It can be further applied to more deep learning tasks such as object detection, image segmentation, and natural language processing. The training efficiency of GPipe can be further improved by better graph partition algorithms.

6. Conclusion

In this work, we introduced GPipe, a scalable model parallelism library that addresses the memory bottleneck for giant neural networks. It allows researchers to explore deeper and more complex deep learning models. For example, GPipe supports models up to $25\times$ larger with 8 accelerators, demonstrating its scalability. Moreover, it can achieve a $3.5\times$ speedup with $4\times$ more accelerators without tuning. In all cases, it converges to identical accuracies as the sequential version without any changes to the model hyperparameters. Furthermore, we demonstrate the power of our framework by training a giant AmoebaNet model that achieves 84.3% top-1 / 97.0% top-5 ImageNet validation accuracy, and pushes the CIFAR-10 accuracy to 99% and CIFAR-100 accuracy 91.3%.

Acknowledgments

We wish to thank Esteban Real, Quoc Le, Xiaodan Song, Alok Aggarwal, Naveen Kumar, Mark Heffernan, Megan Kacholia, Samy Bengio, and Jeff Dean for their support and valuable input; Patrick Nguyen, Xiaoqiang Zheng, Yonghui Wu, Noam Shazeer, Barret Zoph, Ekin Cubuk, Tianqi Chen, Vijay Vasudevan and Ruoming Pang for helpful discussions and inspirations; and the larger Google Brain team.

References

- [1] M. Abadi, P. Barham, J. Chen, Z. Chen, A. Davis, J. Dean, M. Devin, S. Ghemawat, G. Irving, M. Isard, et al. Tensorflow: a system for large-scale machine learning. In *OSDI*, volume 16, pages 265–283, 2016. 3
- [2] T. Berg, J. Liu, S. W. Lee, M. L. Alexander, D. W. Jacobs, and P. N. Belhumeur. Birdsnap: Large-scale fine-grained visual categorization of birds. In *IEEE Conference on Computer Vision and Pattern Recognition*, pages 2019–2026, 2014. 7
- [3] L. Bossard, M. Guillaumin, and L. J. V. Gool. Food-101 - mining discriminative components with random forests. In D. J. Fleet, T. Pajdla, B. Schiele, and T. Tuytelaars, editors, *ECCV 2014*, volume 8694 of *Lecture Notes in Computer Science*, pages 446–461. Springer, 2014. 8
- [4] L. Bottou. Large-scale machine learning with stochastic gradient descent. In *Proceedings of COMPSTAT’2010*, pages 177–186. Springer, 2010. 3
- [5] A. Brock, J. Donahue, and K. Simonyan. Large scale gan training for high fidelity natural image synthesis. *arXiv preprint arXiv:1809.11096*, 2018. 8
- [6] C.-C. Chen, C.-L. Yang, and H.-Y. Cheng. Efficient and robust parallel dnn training through model parallelism on multi-gpu platform. *arXiv preprint arXiv:1809.02839*, 2018. 3
- [7] T. Chen, M. Li, Y. Li, M. Lin, N. Wang, M. Wang, T. Xiao, B. Xu, C. Zhang, and Z. Zhang. Mxnet: A flexible and efficient machine learning library for heterogeneous distributed systems. *arXiv preprint arXiv:1512.01274*, 2015. 3
- [8] T. Chen, B. Xu, C. Zhang, and C. Guestrin. Training deep nets with sublinear memory cost. *arXiv preprint arXiv:1604.06174*, 2016. 2
- [9] X. Chen, A. Eversole, G. Li, D. Yu, and F. Seide. Pipelined back-propagation for context-dependent deep neural networks. In *Thirteenth Annual Conference of the International Speech Communication Association*, 2012. 3
- [10] Y. Chen, J. Li, H. Xiao, X. Jin, S. Yan, and J. Feng. Dual path networks. In *Advances in Neural Information Processing Systems (NIPS)*, pages 4467–4475, 2017. 7
- [11] C.-C. Chiu, T. N. Sainath, Y. Wu, R. Prabhavalkar, P. Nguyen, Z. Chen, A. Kannan, R. J. Weiss, K. Rao, K. Gonina, et al. State-of-the-art speech recognition with sequence-to-sequence models. *arXiv preprint arXiv:1712.01769*, 2017. 1
- [12] C. Coleman, D. Kang, D. Narayanan, L. Nardi, T. Zhao, J. Zhang, P. Bailis, K. Olukotun, C. Re, and M. Zaharia. Analysis of dawnbench, a time-to-accuracy machine learning performance benchmark. *arXiv preprint arXiv:1806.01427*, 2018. 6
- [13] E. D. Cubuk, B. Zoph, D. Mane, V. Vasudevan, and Q. V. Le. Autoaugment: Learning augmentation policies from data. *arXiv preprint arXiv:1805.09501*, 2018. 7, 8
- [14] Y. Cui, Y. Song, C. Sun, A. Howard, and S. Belongie. Large scale fine-grained categorization and domain-specific transfer learning. In *IEEE Conference on Computer Vision and Pattern Recognition*, 2018. 8
- [15] J. Dean, G. Corrado, R. Monga, K. Chen, M. Devin, M. Mao, M. aurelio Ranzato, A. Senior, P. Tucker, K. Yang, Q. V. Le, and A. Y. Ng. Large scale distributed deep networks. In F. Pereira, C. J. C. Burges, L. Bottou, and K. Q. Weinberger, editors, *Advances in Neural Information Processing Systems 25*, pages 1223–1231. Curran Associates, Inc., 2012. 2
- [16] J. Deng, W. Dong, R. Socher, L.-J. Li, K. Li, and L. Fei-Fei. Imagenet: A large-scale hierarchical image database. In *CVPR*, pages 248–255. IEEE, 2009. 1
- [17] J. Devlin, M.-W. Chang, K. Lee, and K. Toutanova. Bert: Pre-training of deep bidirectional transformers for language understanding. *arXiv preprint arXiv:1810.04805*, 2018. 1, 8
- [18] T. DeVries and G. W. Taylor. Improved regularization of convolutional neural networks with cutout. *arXiv preprint arXiv:1708.04552*, 2017. 8
- [19] R. Girshick. Fast r-cnn. In *International Conference on Computer Vision*, pages 1440–1448, 2015. 7
- [20] P. Goyal, P. Dollár, R. Girshick, P. Noordhuis, L. Wesolowski, A. Kyrola, A. Tulloch, Y. Jia, and K. He. Accurate, large minibatch sgd: training imagenet in 1 hour. *arXiv preprint arXiv:1706.02677*, 2017. 8
- [21] A. Griewank and A. Walther. Algorithm 799: revolve: an implementation of checkpointing for the reverse or adjoint mode of computational differentiation. *ACM Transactions on Mathematical Software (TOMS)*, 26(1):19–45, 2000. 2
- [22] A. Harlap, D. Narayanan, A. Phanishayee, V. Seshadri, N. Devanur, G. Ganger, and P. Gibbons. Pipedream: Fast and efficient pipeline parallel dnn training. *arXiv preprint arXiv:1806.03377*, 2018. 3

- [23] K. He, X. Zhang, S. Ren, and J. Sun. Identity mappings in deep residual networks. In *European conference on computer vision*, pages 630–645. Springer, 2016. 2
- [24] J. Hu, L. Shen, and G. Sun. Squeeze-and-excitation networks. *arXiv preprint arXiv:1709.01507*, 2017. 1, 2, 7
- [25] S. Ioffe and C. Szegedy. Batch normalization: Accelerating deep network training by reducing internal covariate shift. *arXiv preprint arXiv:1502.03167*, 2015. 4
- [26] X. Jia, S. Song, W. He, Y. Wang, H. Rong, F. Zhou, L. Xie, Z. Guo, Y. Yang, L. Yu, et al. Highly scalable deep learning training system with mixed-precision: Training imagenet in four minutes. *arXiv preprint arXiv:1807.11205*, 2018. 8
- [27] Y. Jia, E. Shelhamer, J. Donahue, S. Karayev, J. Long, R. Girshick, S. Guadarrama, and T. Darrell. Caffe: Convolutional architecture for fast feature embedding. In *Proceedings of the 22nd ACM international conference on Multimedia*, pages 675–678. ACM, 2014. 3
- [28] S. Kornblith, J. Shlens, and Q. V. Le. Do better imagenet models transfer better? *CoRR*, abs/1805.08974, 2018. 8
- [29] J. Krause, J. Deng, M. Stark, and L. Fei-Fei. Collecting a large-scale dataset of fine-grained cars. In *Second Workshop on Fine-Grained Visual Categorization (FGVC2)*, 2013. 8
- [30] J. Krause, B. Sapp, A. Howard, H. Zhou, A. Toshev, T. Duerig, J. Philbin, and L. Fei-Fei. The unreasonable effectiveness of noisy data for fine-grained recognition. In *ECCV*, 2016. 8
- [31] A. Krizhevsky. One weird trick for parallelizing convolutional neural networks. *arXiv preprint arXiv:1404.5997*, 2014. 3
- [32] A. Krizhevsky and G. Hinton. Learning multiple layers of features from tiny images. *Computer Science Department, University of Toronto, Tech. Rep*, 2009. 7
- [33] V. Kumar, A. Grama, A. Gupta, and G. Karypis. *Introduction to parallel computing: design and analysis of algorithms*, volume 400. Benjamin/Cummings Redwood City, 1994. 3
- [34] S. Lee, J. K. Kim, X. Zheng, Q. Ho, G. A. Gibson, and E. P. Xing. On model parallelization and scheduling strategies for distributed machine learning. In *Advances in neural information processing systems*, pages 2834–2842, 2014. 3
- [35] M. Li, D. G. Andersen, J. W. Park, A. J. Smola, A. Ahmed, V. Josifovski, J. Long, E. J. Shekita, and B.-Y. Su. Scaling distributed machine learning with the parameter server. In *OSDI*, volume 14, pages 583–598, 2014. 3
- [36] D. Mahajan, R. Girshick, V. Ramanathan, K. He, M. Paluri, Y. Li, A. Bharambe, and L. van der Maaten. Exploring the limits of weakly supervised pretraining. *arXiv preprint arXiv:1805.00932*, 2018. 1, 8
- [37] S. Maji, E. Rahtu, J. Kannala, M. B. Blaschko, and A. Vedaldi. Fine-grained visual classification of aircraft. *CoRR*, abs/1306.5151, 2013. 8
- [38] P. Micikevicius, S. Narang, J. Alben, G. Diamos, E. Elsen, D. Garcia, B. Ginsburg, M. Houston, O. Kuchaev, G. Venkatesh, et al. Mixed precision training. *arXiv preprint arXiv:1710.03740*, 2017. 7
- [39] O. M. Parkhi, A. Vedaldi, A. Zisserman, and C. V. Jawahar. Cats and dogs. In *IEEE Conference on Computer Vision and Pattern Recognition*, pages 3498–3505, 2012. 8
- [40] A. Paszke, S. Gross, S. Chintala, G. Chanan, E. Yang, Z. DeVito, Z. Lin, A. Desmaison, L. Antiga, and A. Lerer. Automatic differentiation in pytorch. 2017. 3
- [41] C. Peng, T. Xiao, Z. Li, Y. Jiang, X. Zhang, K. Jia, G. Yu, and J. Sun. Megdet: A large mini-batch object detector. *arXiv preprint arXiv:1711.07240*, 7, 2017. 4
- [42] A. Petrowski, G. Dreyfus, and C. Girault. Performance analysis of a pipelined backpropagation parallel algorithm. *IEEE Transactions on Neural Networks*, 4(6):970–981, Nov 1993. 3
- [43] A. S. Razavian, H. Azizpour, J. Sullivan, and S. Carlsson. Cnn features off-the-shelf: An astounding baseline for recognition. In *IEEE Conference on Computer Vision and Pattern Recognition Workshops*, pages 512–519, 2014. 7
- [44] E. Real, A. Aggarwal, Y. Huang, and Q. V. Le. Regularized evolution for image classifier architecture search. *arXiv preprint arXiv:1802.01548*, 2018. 1, 2, 7
- [45] E. Shelhamer, J. Long, and T. Darrell. Fully convolutional networks for semantic segmentation. *IEEE Trans. Pattern Anal. Mach. Intell.*, 39(4):640–651, 2017. 7
- [46] C. Sun, A. Shrivastava, S. Singh, and A. Gupta. Revisiting unreasonable effectiveness of data in deep learning era. In *Computer Vision (ICCV), 2017 IEEE International Conference on*, pages 843–852. IEEE, 2017. 1, 8
- [47] C. Szegedy, S. Ioffe, V. Vanhoucke, and A. A. Alemi. Inception-v4, inception-resnet and the impact of residual connections on learning. In *AAAI*, 2017. 7
- [48] C. Szegedy, W. Liu, Y. Jia, P. Sermanet, S. Reed, D. Anguelov, D. Erhan, V. Vanhoucke, and A. Rabinovich. Going deeper with convolutions. In *Proceedings of the IEEE conference on computer vision and pattern recognition*, pages 1–9, 2015. 1, 2
- [49] C. Szegedy, V. Vanhoucke, S. Ioffe, J. Shlens, and Z. Wojna. Rethinking the inception architecture for computer vision. In *CVPR*, pages 2818–2826, 2016. 2
- [50] L. G. Valiant. A bridging model for parallel computation. *Communications of the ACM*, 33(8):103–111, 1990. 2, 3
- [51] Y. Wu, M. Schuster, Z. Chen, Q. V. Le, M. Norouzi, W. Macherey, M. Krikun, Y. Cao, Q. Gao, K. Macherey, et al. Google’s neural machine translation system: Bridging the gap between human and machine translation. *arXiv preprint arXiv:1609.08144*, 2016. 3
- [52] S. Xie, R. Girshick, P. Dollár, Z. Tu, and K. He. Aggregated residual transformations for deep neural networks. In *Computer Vision and Pattern Recognition (CVPR), 2017 IEEE Conference on*, pages 5987–5995. IEEE, 2017. 2, 7
- [53] F. Yu, D. Wang, and T. Darrell. Deep layer aggregation. In *IEEE Conference on Computer Vision and Pattern Recognition 2018*, 2018. 8
- [54] X. Zhang, Z. Li, C. C. Loy, and D. Lin. Polynet: A pursuit of structural diversity in very deep networks. In *CVPR*, pages 3900–3908. IEEE, 2017. 7
- [55] Y. Zhang, G. Chen, D. Yu, K. Yaco, S. Khudanpur, and J. Glass. Highway long short-term memory rnns for distant speech recognition. In *Acoustics, Speech and Signal Processing (ICASSP), 2016 IEEE International Conference on*, pages 5755–5759. IEEE, 2016.

- [56] B. Zoph, V. Vasudevan, J. Shlens, and Q. V. Le. Learning transferable architectures for scalable image recognition. *arXiv preprint arXiv:1707.07012*, 2017. [1](#), [2](#), [7](#)